REPORT DOCUMENTATION PAGE

Form Approved OMB NO. 0704-0188

1. REPORT DATE (DD-MM-YYYY)	2. REPORT TYPE	3. DATES COVERED (From - To)
	New Reprint	-

4. TITLE AND SUBTITLE

Low-temperature spin spray deposited ferrite/piezoelectric thin film magnetoelectric heterostructures with strong magnetoelectric coupling

5a. CONTRACT NUMBER
W911NF-09-1-0435

5b. GRANT NUMBER

5c. PROGRAM ELEMENT NUMBER
611103

6. AUTHORS

Z. Zhou, O. Obi, T. X. Nan, S. Beguhn, J. Lou, X. Yang, Y. Gao, M. Li, S. Rand, H. Lin, N. X. Sun, G. Esteves, K. Nittala, J. L. Jones, K. Mahalingam, M. Liu, G. J. Brown

5d. PROJECT NUMBER

5e. TASK NUMBER

5f. WORK UNIT NUMBER

7. PERFORMING ORGANIZATION NAMES AND ADDRESSES

University of Florida Office of Engineering
339 Weil Hall

Gainesville, FL 32611 -6550

8. PERFORMING ORGANIZATION REPORT NUMBER

9. SPONSORING/MONITORING AGENCY NAME(S) AND ADDRESS (ES)

U.S. Army Research Office
P.O. Box 12211
Research Triangle Park, NC 27709-2211

10. SPONSOR/MONITOR'S ACRONYM(S)
ARO

11. SPONSOR/MONITOR'S REPORT NUMBER(S)
54169-MS-PCS.48

12. DISTRIBUTION AVAILIBILITY STATEMENT

Approved for public release; distribution is unlimited.

13. SUPPLEMENTARY NOTES

The views, opinions and/or findings contained in this report are those of the author(s) and should not contrued as an official Department of the Army position, policy or decision, unless so designated by other documentation.

14. ABSTRACT

We report low-temperature spin spray deposited Fe3O4/ZnO thin film microwave magnetic/piezoelectric magnetoelectric heterostructures. A voltage induced effective ferromagnetic resonance field of 14 Oe was realized in Fe3O4/ZnO magnetoelectric (ME) heterostructures. Compared with most thin film magnetoelectric heterostructures

15. SUBJECT TERMS

magnetoelectric, diffraction, thin film

16. SECURITY CLASSIFICATION OF:			17. LIMITATION OF ABSTRACT	15. NUMBER OF PAGES	19a. NAME OF RESPONSIBLE PERSON
a. REPORT	b. ABSTRACT	c. THIS PAGE			Jacob Jones
UU	UU	UU	UU		19b. TELEPHONE NUMBER 919-515-4557

Report Title

Low-temperature spin spray deposited ferrite/piezoelectric thin film magnetoelectric heterostructures with strong magnetoelectric coupling

ABSTRACT

We report low-temperature spin spray deposited Fe3O4/ZnO thin film microwave magnetic/piezoelectric magnetoelectric heterostructures. A voltage induced effective ferromagnetic resonance field of 14 Oe was realized in Fe3O4/ZnO magnetoelectric (ME) heterostructures. Compared with most thin film magnetoelectric heterostructures prepared by high temperature ([600 └C) deposition methods, for example, pulsed laser deposition, molecular beam epitaxy, or sputtering, Fe3O4/ZnO ME heterostructures have much lower deposition temperature (\100 └C) at a much lower cost and less energy dissipation, which can be readily integrated in different integrated circuits.

REPORT DOCUMENTATION PAGE (SF298)
(Continuation Sheet)

Continuation for Block 13

ARO Report Number 54169.48-MS-PCS
Low-temperature spin spray deposited ferrite/pie...

Block 13: Supplementary Note

Approved for public release; distribution is unlimited.

J Mater Sci: Mater Electron (2014) 25:1188 1192
DOI 10.1007/s10854 014 1707 7

Low-temperature spin spray deposited ferrite/piezoelectric thin film magnetoelectric heterostructures with strong magnetoelectric coupling

Z. Zhou · O. Obi · T. X. Nan · S. Beguhn · J. Lou · X. Yang · Y. Gao · M. Li · S. Rand · H. Lin · N. X. Sun · G. Esteves · K. Nittala · J. L. Jones · K. Mahalingam · M. Liu · G. J. Brown

Received: 9 October 2013 / Accepted: 2 January 2014 / Published online: 8 January 2014

Abstract We report low-temperature spin spray deposited Fe_3O_4/ZnO thin film microwave magnetic/piezoelectric magnetoelectric heterostructures. A voltage induced effective ferromagnetic resonance field of 14 Oe was realized in Fe_3O_4/ZnO magnetoelectric (ME) heterostructures. Compared with most thin film magnetoelectric heterostructures prepared by high temperature (>600 °C) deposition methods, for example, pulsed laser deposition, molecular beam epitaxy, or sputtering, Fe_3O_4/ZnO ME heterostructures have much lower deposition temperature (<100 °C) at a much lower cost and less energy dissipation, which can be readily integrated in different integrated circuits.

1 Introduction

Layered magnetoelectric (ME) heterostructures with two or more constituent phases of ferro/ferrimagnetic and piezo/ferroelectric phases have gained a lot of recent interest due to the strong strain mediated ME coupling between the ferro/ferrimagnetic and piezo/ferroelectric phases in ME heterostructures. Magnetoelectric heterostructure enables electric field control of magnetism or vice versa [1 6]. The ME coupling in multiferroics has led to different ME devices, such as picotesla magnetic sensors [7], electric field tunable RF/microwave magnetic devices [8 11], tunable resonators [8], phase shifters [9], tunable inductors [10] and tunable filters [11]. Compared to state of the art microwave magnetic devices tuned by magnetic fields, the electric field or voltage tunable ME devices are much more energy efficient, lightweight, compact, and less noisy.

Studies on ME heterostructures are mostly based on complex oxide piezoelectric ceramic or single crystal, such as lead zirconate titanate, barium titanate, lead zinc niobate lead titanate (PZN-PT), lead magnesium niobate-lead titanate, etc. Most of these thin film ME heterostructures are typically grown by pulsed laser deposition [12], molecular beam epitaxy [13], chemical solution deposition [14], sputtering [5, 6] or pyrolyzing [15]. These deposition methods for ME heterostructures require high processing temperatures of >600 °C, which leads to interface diffusion and degraded RF magnetism or piezoelectricity [14]. The high process temperatures make it very challenging in integrating these ME devices onto radio frequency integrated circuits or monolithic microwave integrated circuits.

Spin-spray deposition method is a unique wet chemical technique for synthesizing high crystalline quality, low-loss and fully dense RF/microwave complex oxide films. For example, spinel ferrites thin film can be fabricated directly from aqueous solution at ~90 °C through this method. The processing temperature is much lower than that of (>600 °C) other ferrite preparation methods [16 18]. In addition, tight atomic bonding can be formed at the interface between spin-spray synthesized ferrite films and

Z. Zhou and O. Obi have contributed equally to this work.

Z. Zhou · O. Obi · T. X. Nan · S. Beguhn · J. Lou · X. Yang · Y. Gao · M. Li · S. Rand · H. Lin · N. X. Sun (✉)
Department of Electrical and Computer Engineering, Northeastern University, Boston, MA 02115, USA
e mail: nian@ece.neu.edu

G. Esteves · K. Nittala · J. L. Jones
Department of Materials Science and Engineering, University of Florida, Gainesville, FL 32611 6400, USA

K. Mahalingam · M. Liu · G. J. Brown
Materials and Manufacturing Directorate, Air Force Research Laboratory, Wright Patterson, AFB, OH 45433 7707, USA

ferroelectrics, with minimal interface inter-diffusion, which leads to strong ME coupling and thereby provides great opportunities for ME heterostructures. Using this method, a giant electric field induced effective magnetic field of 860 Oe has been demonstrated in a Fe_3O_4/PZN-PT magnetic thin film/piezoelectric slab heterostructures [16]. Although spin spray deposition of ferrite films has been widely performed [16], the spin spray deposition of ferroelectrics or piezoelectrics is rarely explored, except for a recent demonstration of a spin spray deposited ZnO films [17, 18]. ZnO is a typical piezoelectric material, which makes it a good candidate for thin film ME heterostructures at low temperatures. ZnO is also a direct wide band gap semiconductor with excellent electrical and optical properties which makes it applicable in a wide variety of electron, optoelectronic, spintronics and nanodevices [17, 18]. The piezoelectric properties of spin spray deposited ZnO films when combined with spin spray deposited ferrites offer a unique opportunity for low-temperature synthesized ferrite/ZnO ME heterostructures, and novel integrated voltage tunable RF/microwave ME devices.

In this communication, we demonstrate ME ferrite/piezoelectric thin film heterostructures of Fe_3O_4 (1.4 μm)/ZnO (3 μm) fabricated by the spin-spray process on a glass substrate. A clean interface with negligible inter-diffusion between Fe_3O_4 and ZnO layers was obtained from the low-temperature deposition, which led to a tight interface bonding and strong ME coupling. This is in sharp contrast to other ME heterostructures deposited by other high-temperature deposition methods above [5, 6, 12 15]. Strong static and microwave ME interactions were observed in the Fe_3O_4/ZnO ME heterostructure. A large voltage induced effective magnetic field of 14 Oe was observed through voltage induced in-plane ferromagnetic resonance (FMR) field shift in the Fe_3O_4/ZnO heterostructures. Compared to the high process temperature of >600 °C involved in the deposition process of these thin film heterostructures [12, 13], this low temperature spin-spray processing fabricated ME heterostructures provide a viable route to integration of complex oxide thin film ME structures on integrated circuits.

2 Experiment

Fe_3O_4 (1.4 μm)/ZnO (3 μm) magnetoelectric ferrite/piezoelectric thin film heterostructures fabricated by the spin-spray process on a glass substrate (0.2 mm). The Fe_3O_4/ZnO heterostructure composition was confirmed by X-ray diffraction (XRD) patterns using conventional Bragg Brentano diffraction geometry. The cross-section of Fe_3O_4/ZnO structure was determined by energy-filtered transmission electron microscope (EFTEM) imaging. The crystallographic texture of the thin film Fe_3O_4 (1.4 μm)/ZnO (3 μm) heterostructure was further investigated via XRD at beam-line 11-ID-C of the Advanced Photon Source [19 21] using an X-ray wavelength of $\lambda = 0.10804$ Å. Static ME coupling of thin films Fe_3O_4/ZnO ME heterostructures was investigated by electric-field induced changes in a vibrating sample magnetometer (VSM). Piezoelectric coefficient of ZnO film was obtained by a photonic sensor. Microwave ME coupling of thin films Fe_3O_4/ZnO heterostructures was carried out by custom-made microwave FMR spectrometer.

3 Results and discussion

3.1 Characterization of Fe_3O_4/ZnO thin films heterostructure

Figure 1a shows the XRD patterns of Fe_3O_4/ZnO heterostructure. A clear polycrystalline spinel ferrite phase and a typical ZnO wurtzite structure with no strong preferred orientation is apparent in the Fe_3O_4 and ZnO films. Figure 1b is an EFTEM image showing the ZnO/Fe_3O_4 structure in cross-section. The EFTEM imaging was performed based on the three-window technique [22]. This is a composite (RGB) image constructed by superimposing two independent maps of Fe (green) and Zn (red) distribution across the whole structure. A sharp boundary distinguishing the two layers is evident, indicating insignificant inter-diffusion at the interface. This is also supported by further examination of this region by high-resolution transmission electron microscopy, shown in Fig. 1c, which reveals the presence of an abrupt and well defined interface between the ZnO and Fe_3O_4 layers.

The crystallographic texture of the thin film Fe_3O_4 (1.4 μm)/ZnO (3 μm) heterostructure was further investigated via XRD at beam-line 11-ID-C of the Advanced Photon Source [19 21] using an X-ray wavelength of $\lambda = 0.10804$ Å. The measured diffraction image is shown in Fig. 2a and a 2θ section is extracted from 2.1° to 6.2° over the azimuthal angle from 0° to 180° and shown in Fig. 2b. The positions of the ZnO, Fe_3O_4 and copper diffraction intensities are also indicated at the top of Fig. 2b for complete phase identification. The ZnO (10.0) diffraction intensities are observed at the lowest 2θ position (corresponding to an inter-planar distance, or d, of 2.81 Å) and the ZnO (00.2) diffraction intensities are observed at the next highest 2θ position (d = 2.603 Å). Both ZnO (10.0) and (00.2) are non-uniform with azimuthal angle, with the (10.0) intensity being concentrated around azimuthal angles of 0° and 180° (parallel to the plane of the film) and the (00.2) intensity being concentrated around an azimuthal angle of 90° (in the direction normal to the film).

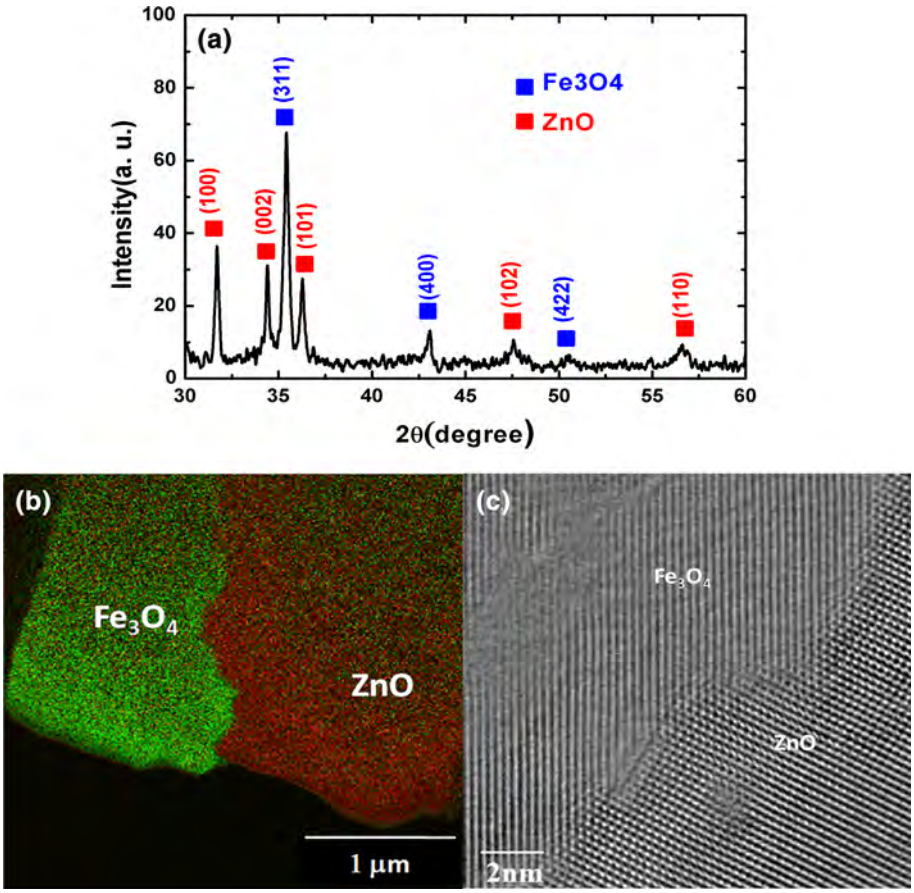

Fig. 1 **a** X ray diffraction pattern of the spin spray deposited Fe3O4/ZnO thin films ME composite; **b** Energy Filtered TEM image showing the zinc oxide (*red*) and iron oxide (*green*) layers; **c** HRTEM image of the iron oxide/zinc oxide interface (Color figure online)

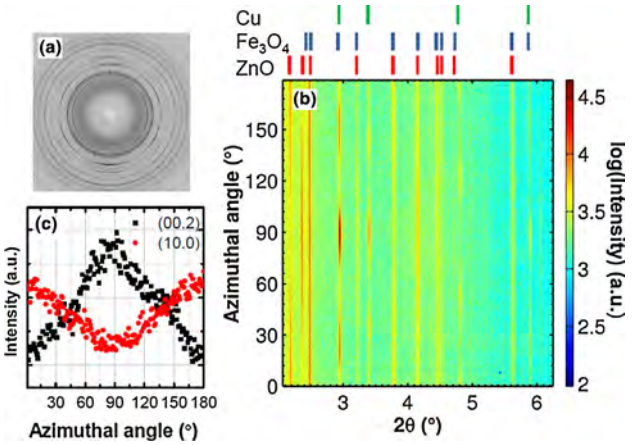

Fig. 2 **a** The measured X ray diffraction image using high energy X rays in transmission geometry; **b** a 2θ section from 2.1° to 6.2° over the azimuthal angle from 0° to 180°; **c** the distribution of the ZnO (10.0) and (00.2) diffraction intensities over the azimuthal angle of the detector were extracted and are presented

The distribution of the ZnO (10.0) and (00.2) diffraction intensities over the azimuthal angle of the detector were extracted and are presented in Fig. 2c. These intensity distributions indicate that the ZnO film is 00.*h*-type fiber textured. To quantify the strength of the ZnO (00.*h*) texture, peak fitting was performed on the (00.*h*) peak using the curve fitting toolbox in MATLAB© (version R2011b) and the full width at half maximum of this diffraction peak is determined to be 76° ± 4.8°.

3.2 Static ME coupling measurements of Fe_3O_4/ZnO heterostructure

Static ME coupling of thin films Fe_3O_4/ZnO ME heterostructures was investigated by electric-field induced changes in a VSM for magnetic hysteresis loops measurements as shown in Fig. 3a, b. This was done by applying an external electric-field (E-field) perpendicular to the ZnO film plane (that is, through the thickness direction). The E-field applied to the ZnO thin film led to strain/stress in the Fe_3O_4/ZnO heterostructure. Magnetization changes were created by the electric-field induced strain due to the inverse magneto-elastic effect. Therefore, electric-field tuning of magnetization can be realized in the ME heterostructure composites through the strain/stress mediated ME coupling.

Figure 3a shows the magnetic hysteresis under different voltages from −20 to 20 V, corresponding to ± 67 kV/cm electric field (E-field), applied across the thickness

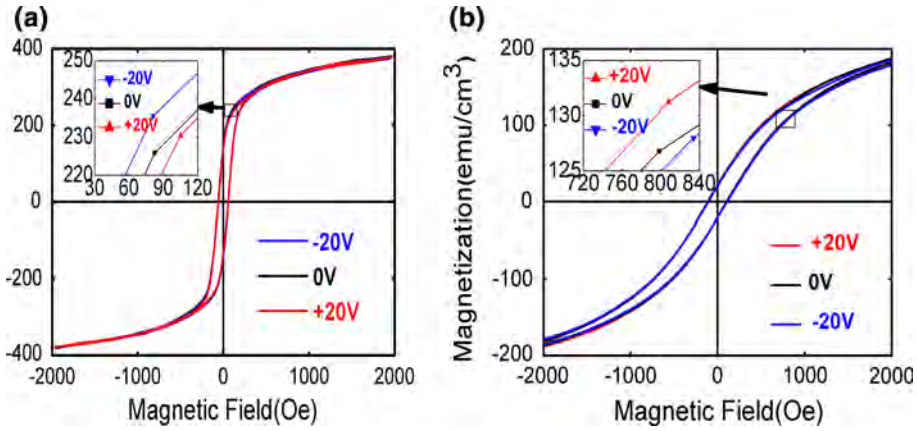

Fig. 3 **a** In plane magnetic hysteresis loops of the Fe3O4/ZnO ME heterostructure under different electric voltages. **b** Out of plane magnetic hysteresis loops of the Fe3O4/ZnO ME heterostructure. The enlarged ME coupling hysteresis loop shift is shown on *upper left inset* on both figures

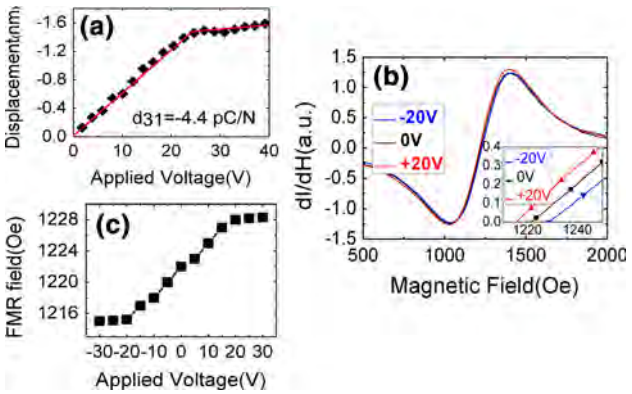

Fig. 4 **a** Piezoelectric coefficient measurements of ZnO thin film; **b** electric field dependence of the in plane field sweep FMR spectra of the Fe3O4/ZnO ME heterostructure measured at 9.3 GHz. The zero cross part was enlarged to demonstrate a clear ME coupling shift at *bottom right inset*; **c** X band in plane ferromagnetic resonance (FMR) field of the Fe3O4/ZnO heterostructure measured at varying applied voltages across the ZnO layer

direction of the ZnO layer, which is about $\Delta M/M = 6.5$ % under a constant bias field of 100 Oe. The electric field induced magnetization change is small due to the substrate clamping effect, thin thickness of the ZnO (3.0 μm) and small piezoelectric coefficient of ZnO, $d_{33} = 10.1$ pC/N, $d_{31} = -5.0$ pC/N, [18] which lead to a relatively small ME coupling coefficient. Figure 3b demonstrated out-of-plane magnetic hysteresis under different electric field induced ME coupling, which indicated ΔM/M = 1.9 % at a bias field of 840 Oe.

Piezoelectric coefficient of ZnO film was obtained by measuring the substrate bending effect [23]. Upon applying an electric field, substrate bending can be anticipated in ZnO/glass heterostructure. Assuming one side of the specimen is fixed, the bending displacement δ can be calculated as [23]:

$$\delta = \frac{1}{2}\kappa L^2 = \frac{L^2}{2t_p}\frac{6AB(1+B)}{A^2B^4 + 2A(2B+3B^2+2B^3)+1}\cdot d_{31}E_3 \quad (1)$$

where κ is curvature, $A = Y_S/Y_P$, $B = t_S/t_P$, Y_S is the Young's modulus of the glass substrate layer ($Y_S = 48$ GPa), Y_P is the Young's modulus of ZnO piezoelectric layer ($Y_P = 17$ GPa), tS the thickness of the glass substrate layer ($t_S = 0.2$ mm) and tP the thickness of the piezoelectric layer (Electric field E_3 was applied along ZnO thickness direction. The sample was cut into length $L = 2$ cm, width of 0.5 cm. By using a photonic sensor, small displacement δ can be measured for determining substrate bending quantitatively. Furthermore, as shown on Fig. 4a, we can calculate piezoelectric coefficient d_{31} through the relationship of $\delta(E)$. From Eq. (1), we get the measured d_{31} of the ZnO thin film, as shown in Fig. 4b, fitted by red curve, in the Fe_3O_4/ZnO ME heterostructure is −4.4 pC/N, which is close to theory value of −5.0 pC/N [17, 18].

3.3 Microwave ME coupling measurements of Fe_3O_4/ZnO heterostructure

Microwave ME interactions and magnetic tunabilities of the Fe_3O_4/ZnO multilayer were demonstrated by electrostatic-field-induced in-plane FMR field changes at room temperature, as shown in Fig. 4a. Here, a custom-made microwave FMR spectrometer using a planar transmission line was used to perform the FMR measurements of the ferrite/ferroelectric ME thin films composites at X-band (9.3 GHz). In Fig. 4a, the bias magnetic field, was applied in the Fe_3O_4/ZnO film plane with in-plane the microwave RF field and was perpendicular to the DC bias field. A clear electric field induced effective magnetic field 14 Oe, correspondingly, was observed between a bias voltage of −20 and 20 V, which is indicated by the electric field induced FMR field change, as shown in bottom right inset of Fig. 4b. Figure 4c shows the FMR field dependence of applied voltage from −30 to 30 V. The FMR field varies linearly as applied voltage switches from −20 to 20 V, indicating the piezoelectric property of ZnO thin film. The FMR field, however, saturates as applied voltage is larger

than 20 V, this result accords with the piezoelectric measurement of ZnO in Fig. 4a, where the displacement of ZnO/glass substrate linearly increases as applied voltage from 0 to 23 V, however, saturated around 23 V. This phenomenon is reasonable because the FMR field won't increase to infinite as applied voltage increase. The Fe_3O_4/ZnO heterostructure, can be considered as capacitance, has breakdown voltage limit, which is 23 V in our experiment.

This electric-field-induced FMR field change can be explained by the strain-mediated electrostatic-field-induced magnetic anisotropy field H_{eff}. The E-field applied across ZnO layer can tune the FMR field of Fe_3O_4 layer up or down through strain/stress mediated ME coupling [5, 6], see Fig. 4b. The in-plane FMR frequency can be expressed by the well-known Kittel equation [6]:

$$f = \gamma\sqrt{(H_r + H_k + H_{eff})(H_r + H_k + H_{eff} + 4\pi M_s)} \qquad (2)$$

where γ is the gyromagnetic constant (2.8 MHz/Oe), f is resonance frequency of 9.3 GHz, H_r is the FMR field, H_k is the anisotropic field in plane, $4\pi M_s$ is the magnetization of 5,100 Gauss. $H_{eff} = 3\lambda_S Y d_{31} E_3/M_S$ is the E-field induced effective in-plane magnetic field, where, Y is Young's Modulus of Fe_3O_4 (2.3×10^7 N m^{-2}), λ_S (28 ppm) is the saturate magnetostriction constant of Fe_3O_4 at 250 Oe bias magnetic field [24]. In addition, FMR frequency spectrum was measured by applying a voltage on ZnO from −30 to 30 V. We can easily calculate the theoretical $H_{eff} = 30$ Oe and the corresponding ME coupling coefficient $\alpha = \Delta H_{eff}/\Delta E$ is 3.0×10^{-4} Oe cm k/V, larger than measured H_{eff} of 14 Oe and α of 1.4×10^{-4} Oe cm k/V. The reason is thickness of glass substrate (0.2 mm) is much larger than piezoelectric layer (3 μm), therefore, reduced ME coupling effect due to substrate clamping effect significantly [12, 13].

4 Conclusion

In conclusion, novel magnetic/piezoelectric thin film ME heterostructures of Fe_3O_4 (1.4 μm)/ZnO (3 μm) on glass substrate were fabricated, which showed a strong ME coupling. A diffusion-free, and well defined interface between iron oxide and zinc oxide layers was achieved due to the low temperature spin spray deposition process. A significant voltage induced in-plane resonance magnetic field shift ΔH_{eff} of 14 Oe was observed, corresponding to ME coupling coefficient $\alpha = \Delta H_{eff}/\Delta E = 1.5 \times 10^{-4}$ Oe cm k/V. Firstly, low temperature spin-spray deposition technology was confirmed as a good synthesis method for depositing thin films ME heterostructures. Secondly, a relative large strain induced FMR frequency shift of 14 Oe was shown in thin film heterostructures compared to other thin films ME structure with ME coupling of 5 6 Oe [12, 13]. This work paved the way for potential multifunctional ZnO-based E-field tuning microwave/RF devices.

Acknowledgments This work is financially supported by NSF CAREER awards 0746810 and by the United States Air Force Research Laboratory under contract number FA8721 05 C 0002. J.J., K.N., and G.E. acknowledge support from the Army Research Office through contract number W911NF 09 1 0435. Use of the Advanced Photon Source, an Office of Science User Facility operated for the U.S. Department of Energy (DOE) Office of Science by Argonne National Laboratory, was supported by the U.S. DOE under Contract No. DE AC02 06CH11357.

References

1. W. Eerenstein, N.D. Mathur, J.F. Scott, Nature **442**, 759 (2006)
2. C.W. Nan, M.I. Bichurin, S.X. Dong, D. Viehland, G. Srinivasan, J. Appl. Phys. **103**, 1101 (2008)
3. C.A.F. Vaz, J. Hoffman, C.H. Ahn, R. Ramesh, Adv. Mater. **22**, 2900 2918 (2010)
4. H. Zheng, J. Wang, S.E. Lofland, Z. Ma, L. Mohaddes Ardabili, T. Zhao, L. Salamanca Riba, S.R. Shinde, S.B. Ogale, F. Bai, D. Viehland, Y. Jia, D.G. Schlom, M. Wuttig, A. Roytburd, R. Ramesh, Science **303**, 661 663 (2004)
5. Z. Zhou, S. Beguhn, J. Lou, S. Rand, M. Li, X. Yang, S.D. Li, M. Liu, N.X. Sun, J. Appl. Phys. **111**, 103915 (2012)
6. M. Liu, Z. Zhou, T. Nan, B.M. Howe, G.J. Brown, N.X. Sun, Adv. Mater. **25**, 1435 (2013)
7. S.X. Dong, J.F. Li, D. Viehland, Appl. Phys. Lett. **83**, 2265 (2003)
8. T.X. Nan, Y. Hui, M. Rinaldi, N.X. Sun, Scientific Rep. **3**, 1985 (2013)
9. G.M. Yang, J. Lou, O. Obi, N.X. Sun, IEEE Microw. Wirel. Compon. Lett. **21**, 240 (2011)
10. J. Lou, D. Reed, M. Liu, N.X. Sun, Appl. Phys. Lett. **94**, 112508 (2009)
11. X. Yang, J. Wu, S. Beguhn, T. Nan, Y. Gao, Z. Zhou, N.X. Sun, IEEE Microw. Wirel. Compon. Lett. **23**, 184 (2013)
12. Z. Li, Y. Gao, B. Yang, Y.H. Lin, R. Yu, C.W. Nan, J. Am. Ceram. Soc. **94**, 1060 (2011)
13. Jaydip Das, Young Yeal Song, Nan Mo, Pavol Krivosik, Carl E. Patton, Adv. Mater. **21**, 2045 (2009)
14. N. Li, M. Liu, Z.Y. Zhou, N.X. Sun, D.V.B. Murthy, G. Srinivasan, T.M. Klein, V.M. Petrov, A. Gupta, Appl. Phys. Lett. **99**, 192502 (2011)
15. Z. Li, J.M. Hu, L. Shu, Y. Gao, Y. Shen, Y.H. Lin, C.W. Nan, J. Appl. Phys. **111**, 033918 (2012)
16. M. Liu, O. Obi, J. Lou, S. Stoute, J.Y. Huang, Z.H. Cai, K.S. Ziemer, N.X. Sun, Appl. Phys. Lett. **92**, 152504 (2008)
17. Ü. Özgür, Y.I. Alivov, C. Liu, A. Teke, M A. Reshchikov, S. Doğan, V. Avrutin, S.J. Cho, H. Morkoçd, J. Appl. Phys. **98**, 041301 (2005)
18. H. Wagata, N. Ohashi, T. Taniguchi, K. Katsumata, K. Okada, N. Matsushita, Cryst. Growth Des. **10**, 4968 (2011)
19. G. Tutuncu, M. Motahari, J. Bernier, M. Varlioglu, J. L. Jones, E. Ustundag, J. Am. Ceram. Soc. 1 (2012)
20. T.M. Usher, J.S. Forrester, C.R. dela Cruz, J.L. Jones, Appl. Phys. Lett. **101**, 152906 (2012)
21. G. Leighton, Z.R. Huang, Smart Mater. Struct. **19**, 065011 (2010)
22. F. Hofer and P. Warbichler, Ed. C. C. Ahn, 2nd edn (Wiley VCH, Darmstadt, 2004), pp. 159 222
23. R. L. Johnson, Master Thesis, Iowa State University (2005)
24. N. Izyumskaya, V. Avrutin, X. Gu, B. Xiao, S. Chevtchenko, J.G. Yoon, H. Morkoc, L. Zhou, D.J. Smith, Appl. Phys. Lett. **91**, 182906 (2007)